IMMUNOLOGY

Gammaherpesvirus infection drives age-associated B cells toward pathogenicity in EAE and MS

Isobel C. Mouat[1,2], Jessica R. Allanach[2], Naomi M. Fettig[2], Vina Fan[2,3], Anna M. Girard[2,3], Iryna Shanina[2], Lisa C. Osborne[2], Galina Vorobeychik[4,5], Marc S. Horwitz[2]*

While age-associated B cells (ABCs) are known to expand and persist following viral infection and during autoimmunity, their interactions are yet to be studied together in these contexts. Here, we directly compared CD11c$^+$T-bet$^+$ ABCs using models of Epstein-Barr virus (EBV), gammaherpesvirus 68 (γHV68), multiple sclerosis (MS), and experimental autoimmune encephalomyelitis (EAE), and found that each drives the ABC population to opposing phenotypes. EBV infection has long been implicated in MS, and we have previously shown that latent γHV68 infection exacerbates EAE. Here, we demonstrate that ABCs are required for γHV68-enhanced disease. We then show that the circulating ABC population is expanded and phenotypically altered in people with relapsing MS. In this study, we show that viral infection and autoimmunity differentially affect the phenotype of ABCs in humans and mice, and we identify ABCs as functional mediators of viral-enhanced autoimmunity.

INTRODUCTION

Age-associated B cells (ABCs), also referred to as atypical B cells, are a unique subset of B cells found in humans and mice. They have been identified and characterized independently in the contexts of female aging, viral infection, and autoimmunity (*1*–*3*). In life, these are overlapping and intertwined occurrences. ABCs, defined by high expression of CD11c and T-bet and low expression of CD21, are primarily found in the spleen and secrete antiviral antibodies, autoantibodies, and cytokines and act as antigen-presenting cells (APCs) (*1*, *4*, *5*). The number of ABCs increases with age, particularly in females (*3*, *6*–*10*). ABC numbers are also increased in people with autoimmune diseases, including systemic lupus erythematosus (SLE), rheumatoid arthritis (RA), and multiple sclerosis (MS), and in a subset of people with common variable immunodeficiency that display autoimmune complications (*3*, *6*, *7*, *9*–*13*). In a mouse model of SLE, knocking out T-bet specifically in B cells impairs the development of germinal centers, decreases autoantibody levels, and dampens kidney damage and mortality (*14*). ABCs have been shown to produce the proinflammatory cytokines interferon-γ (IFNγ) and tumor necrosis factor–α (TNFα) as well as the regulatory cytokine interleukin-10 (IL-10) in autoimmune contexts (*4*, *15*). ABCs also expand in an array of viral infections including lymphocytic choriomeningitis virus (LCMV), murine cytomegalovirus (MCMV), gammaherpesvirus68 (γHV68), vaccinia, HIV, influenza, hepatitis C, and rhinovirus (*2*, *16*–*23*). ABCs have primarily been examined separately in the contexts of viral infection and autoimmunity. Given the distinct pathologies of viral infections and autoimmunity, we would expect that ABCs would take on distinct phenotypes and functional capacities depending on the nature of the immune stimulus. Recently, ABCs in people with HIV and SLE were shown to have similar but not completely overlapping transcriptional profiles (*24*). The phenotypic and functional characteristics of ABCs between disease states deserve further investigation. To our knowledge, ABCs have yet to be examined in the in vivo MS model experimental autoimmune encephalomyelitis (EAE), although ABC differentiation depends on T-bet, a transcription factor that is essential for EAE (*25*). The functional capacities of ABCs and their contribution(s) to MS and EAE are not well understood. Here, we do a side-by-side comparison of the ABC population in the contexts of viral infection and autoimmunity in both mice and humans to ascertain the specific interactions driven by these two processes and their relative roles in disease progression. Specifically, we examine the role of ABCs as mediators between gammaherpesvirus infection and MS/EAE.

Epstein-Barr virus (EBV) is a highly prevalent human gammaherpesvirus that establishes latency in B cells. EBV infects more than 90% of the adult population and is considered a causative agent of MS (*26*). The association between EBV and autoimmune disease was first demonstrated in 1979 when it was reported that peripheral blood lymphocytes from MS patients have an increased tendency to transform in vitro in response to EBV (*27*). Epidemiological findings support the association between EBV and MS; EBV is present in nearly 100% of people with MS, and seronegativity protects from disease (*28*–*30*). There is geographic overlap of infectious mononucleosis (IM), an immune system–driven syndrome usually caused by EBV, and MS (*31*), and a history of IM increases risk of developing MS (*32*, *33*). A recent paper used U.S. military records of more than 10 million young adults to demonstrate that EBV infection precedes MS development and that EBV infection, but not other viral infections, increases the risk of MS development 32-fold (*34*). There is also robust clinical evidence for EBV's contribution to MS. People with MS have higher titers of EBV-specific antibodies than healthy individuals (*35*), which correlate with disease activity (*36*), anti-EBV titers in the cerebrospinal fluid are elevated in those with MS (*37*), and T cells in people with MS display aberrant responses to EBV (*38*). Further work has demonstrated that EBV's association with autoimmune disease extends to SLE and RA (*39*–*44*). The precise mechanism of EBV's contribution to MS is incompletely understood, although multiple possible mechanisms have been

[1]Centre for Inflammation Research, University of Edinburgh, Edinburgh, UK. [2]Department of Microbiology and Immunology, University of British Columbia, Vancouver, British Columbia, Canada. [3]Department of Medicine, University of Calgary, Calgary, Alberta, Canada. [4]Fraser Health Multiple Sclerosis Clinic, Burnaby, British Columbia, Canada. [5]Division of Neurology, Department of Medicine, University of British Columbia, Vancouver, British Columbia, Canada.
*Corresponding author. Email: mhorwitz@mail.ubc.ca

proposed, including EBV infection of autoreactive B cells, molecular mimicry, bystander activation of autoreactive cells, EBV-infected B cell invasion of the central nervous system (CNS) and activation of human endogenous retrovirus-W, and EBV-induced cytokine response (*45*, *46*).

Our group has previously demonstrated that infection with latent γHV68, a murine model of EBV (*47*), exacerbates myelin oligodendrocyte glycoprotein peptide ($MOG_{35–55}$)–induced EAE in C57BL/6(J) mice, provoking pathology more reminiscent of MS than in uninfected EAE mice (*48*). Mice latently infected with γHV68 display an earlier and more severe EAE clinical course with increased demyelination, although without viral reactivation or CNS infection. Latent γHV68-infected EAE mice have a heightened peripheral CD8 T cell response and develop CNS lesions composed of both $CD4^+$ and $CD8^+$ T cells, with a proportion of infiltrating $CD8^+$ T cells specific for γHV68. Disease enhancement is dependent on the development of latency and is specific to γHV68; other viral infections, including LCMV and MCMV, do not lead to EAE enhancement (*49*). This γHV68-EAE model is a valuable model of the relationship between EBV and MS, and here, we demonstrate that the specific induction of ABCs is required for the latent γHV68-mediated enhancement of EAE. We propose that alteration of the ABC population due to gammaherpesvirus infection is a mechanism by which viral infection contributes to the development and progression of autoimmune disease.

RESULTS

γHV68 infection and EAE induction expand ABC populations

To determine whether ABCs are differentially affected by gammaherpesvirus infection in an in vivo model of MS, we examined the proportion of ABCs following latent γHV68 infection and EAE induction. We examined the relative proportions of ABCs in C57BL/6(J) mice mock-infected (naïve), infected with γHV68 for 35 days (γHV68), or induced for EAE with $MOG_{35–55}$ (EAE). We also examined ABCs in the γHV68-EAE model, wherein mice were infected with γHV68 for 35 days and subsequently induced for $MOG_{35–55}$ EAE (γHV68-EAE). Spleens, brains, spinal cords, and cervical lymph nodes (CLNs) were collected and processed for flow cytometry (fig. S1A). We asked whether the abundance of ABCs in the spleen changes with γHV68 infection, with EAE induction, or in γHV68-EAE mice, and whether ABCs are found at the site of disease, the CNS, or draining CLNs during EAE.

Unexpectedly, we observed increased proportions of ABCs in females compared to males following both γHV68 infection and EAE induction. While γHV68 infection increases the relative proportion of ABCs among immunoglobulin D–negative (IgD^-) B cells in the spleen of both male and female mice, induction of EAE increases the proportion of ABCs only in females (Fig. 1, A and B). During γHV68-EAE, the proportion of ABCs is increased compared to naïve mice in both females and males (Fig. 1, A and B). The proportion of ABCs is increased in females as compared to males in γHV68, EAE, and γHV68-EAE mice, although there is no initial sex bias observed in naïve mice (Fig. 1, C to F). We did not observe a difference in T-bet expression in splenic ABCs between groups (fig. S1B). Total numbers of ABCs in the spleen also display a sex bias, with increased numbers in females compared to males during EAE and γHV68-EAE (fig. S1C). The female sex bias observed is a surprise because a sex bias has not been observed in $MOG_{35–55}$ EAE in C57BL/6 mice previously (*50*, *51*), nor has a sex difference been reported in γHV68 infection.

We asked whether γHV68 infection or EAE leads to changes in ABC numbers within the CNS, the site of disease during EAE. Not surprisingly, in naïve and γHV68-infected mice, without EAE induction, we did not observe increased numbers of ABCs in the brain or spinal cord, consistent with low overall presence of immune cells in the non-EAE CNS (Fig. 1, G and H). However, EAE induction increased the number of ABCs in the brain and spinal cord in both uninfected and γHV68-infected mice (Fig. 1, G and H). We also observed a trend toward increased proportions of ABCs in the CLNs during EAE and γHV68-EAE (fig. S1D). We found that ABCs constitute a lower proportion of total leukocytes in the brain, spinal cord, and CLNs compared to the spleen (fig. S1E). The precise localization of the CNS-infiltrating ABCs is not known, and whether they localize in the meninges or parenchyma or associate with lesions or ectopic lymphoid structures could give insight into their role within the CNS during disease. However, the low numbers of ABCs occurring in the CNS will likely pose technical challenges. Unlike in the spleen, we did not observe a difference in the number of ABCs within the CNS between males and females (Fig. 1, I and J).

These findings demonstrate that ABCs display a sex bias in the contexts of viral infection and autoimmunity and support previous findings that ABCs are largely resident in the spleen. To further investigate the role(s) of ABCs in viral infection and autoimmunity, we next examined the phenotype of ABCs in these different contexts.

γHV68 infection and EAE differentially affect the ABC phenotype

Previous reports have demonstrated that ABCs display a unique phenotype from other B cell populations (*1*). To examine the ABC phenotype in comparison to non-ABC B cells during γHV68 infection and EAE, we performed flow cytometry on ABCs ($CD11c^+T\text{-}bet^+$) and non-ABCs ($CD11c^-T\text{-}bet^+$) in the spleen (Fig. 2A). In line with previous findings, we observed that ABCs displayed a distinct phenotype from non-ABCs in naïve mice and during γHV68, EAE, and γHV68-EAE (Fig. 2B). In particular, ABCs displayed up-regulated expression of various cytokines, including IFNγ, TNFα, IL-17A, and IL-10, compared to non-ABCs (Fig. 2B). However, not all cytokines were up-regulated on ABCs; the percentage of ABCs expressing IL-6 and granulocyte-macrophage colony-stimulating factor (GM-CSF) was comparable to non-ABC B cells and ABCs expressed less BAFF than non-ABCs (fig. S2, A to C), aligning with previous findings that ABCs do not require BAFF stimulation for persistence (*1*). In addition, various markers previously associated with ABCs displayed increased expression, including CD27, PD1, IDO and Fas, and CTLA4 and PDL1 expression increased on ABCs compared to non-ABCs only during γHV68 infection (Fig. 2B, fig. S2, and table S1).

Although ABCs are implicated in both viral infection and autoimmunity, to our knowledge, the ABC phenotype has not been directly compared in these two instances. To compare how γHV68 infection and EAE induction influence the ABC phenotype, we examined extracellular and intracellular markers on splenic ABCs from EAE mice with and without previous γHV68 infection. Preliminary analysis found no significant differences in the ABC

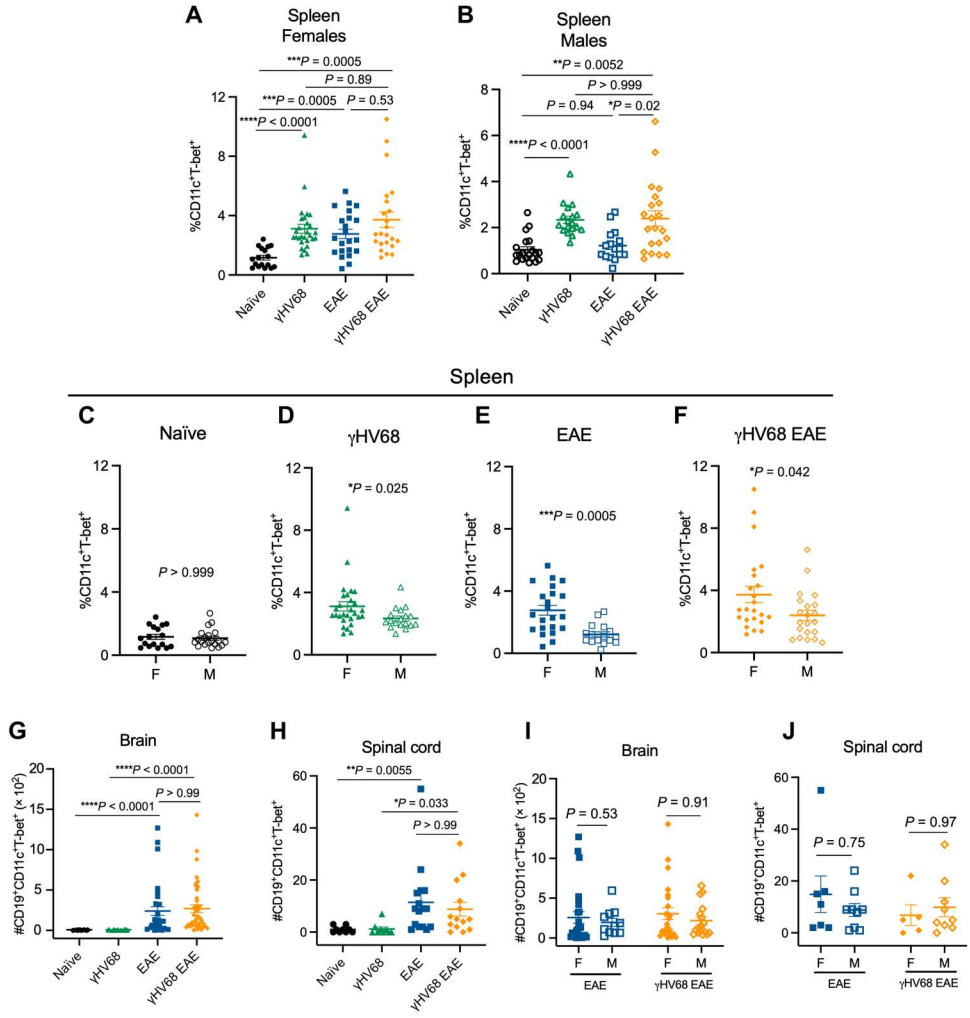

Fig. 1. ABCs are expanded in a sex-biased manner during γHV68 infection and EAE. C57BL/6(J) mice were infected with γHV68 for 35 days to establish latency (γHV68, green triangles) or mock-infected with blank medium (naïve, black circles). In some mice, $MOG_{35–55}$ EAE was induced 35 days after mock infection (EAE, blue squares) or initial virus infection (γHV68 EAE, orange diamonds). At 35 days post-infection (p.i.) or 13 days after EAE induction, spleens, brains, and spinal cords were collected and processed for flow cytometry. (**A** and **B**) Proportion of ABCs ($CD11c^+T\text{-}bet^+$) of previously activated B cells ($CD19^+IgD^-$) in the spleen of females (filled symbols) and males (open symbols). (**C** to **F**) Proportion of ABCs ($CD11c^+T\text{-}bet^+$) of previously activated B cells ($CD19^+IgD^-$) in the spleen of females (F) and males (M). Data are repeated from (A) and (B) in (C) to (F) for better visualization and comparison of sex differences. (**G** and **H**) Number of ABCs in the brain (G) and spinal cord (H), data from both male and female mice. (**I** and **J**) Number of ABCs in the brain (I) and spinal cord (J) of induced mice, separated by males (M) and females (F). Data repeated from (G) and (H) with sex are indicated. (A to F) Data pooled across nine experiments; $n = 16$ to 29 mice per group. (G to J) Data pooled across five experiments; $n = 9$ to 41 mice per group. Data are presented as means ± SEM, analyzed by one-way analysis of variance (ANOVA; A and B), Mann-Whitney (C to F, I, and J), or Kruskal-Wallis (G and H) test; $^{****}P < 0.0001$, $^{***}P < 0.001$, $^{**}P < 0.01$, and $^{*}P < 0.05$.

phenotype between females and males, although a trend toward altered PDL1 expression in males warrants further investigation (fig. S3, A to C). For the purposes of this study, we focused our analysis on female mice.

We found that γHV68 infection and EAE induction each drive differential ABC phenotypes that are distinct from one another and from the ABC phenotype of naïve mice. Specifically, γHV68 infection led to an increase in the proportion of ABCs expressing IFNγ and TNFα, and a decrease in ABCs expressing IL-17A (Fig. 2, C and D). In contrast, EAE results in an increased proportion of ABCs expressing IL-17A and IL-10, and no change in IFNγ or TNFα, compared to ABCs in naïve mice (Fig. 2, C and D). Furthermore, γHV68 infection results in significantly fewer ABCs expressing the inhibitory receptors CTLA4, PDL1, and IDO, while EAE increases the proportion of ABCs expressing CTLA4, PD1, and PDL1 (Fig. 2E and fig. S3). The proportion of ABCs expressing Fas appeared unchanged by γHV68 infection or EAE (Fig. 2E and fig. S3). γHV68 infection increased the proportion of ABCs expressing CD27, while EAE did not (Fig. 2E and fig. S3).

We also asked how γHV68 infection before EAE induction affects the phenotype of ABCs. We observed that previous latent infection with γHV68 drives ABCs toward a T helper 1 (T_H1) phenotype during EAE. In particular, ABCs in γHV68-EAE mice displayed increased IFNγ positivity compared to those from EAE mice (Fig. 2, C to E). These results suggest that ABCs take on a regulatory-like phenotype during EAE, with elevated expression of IL-

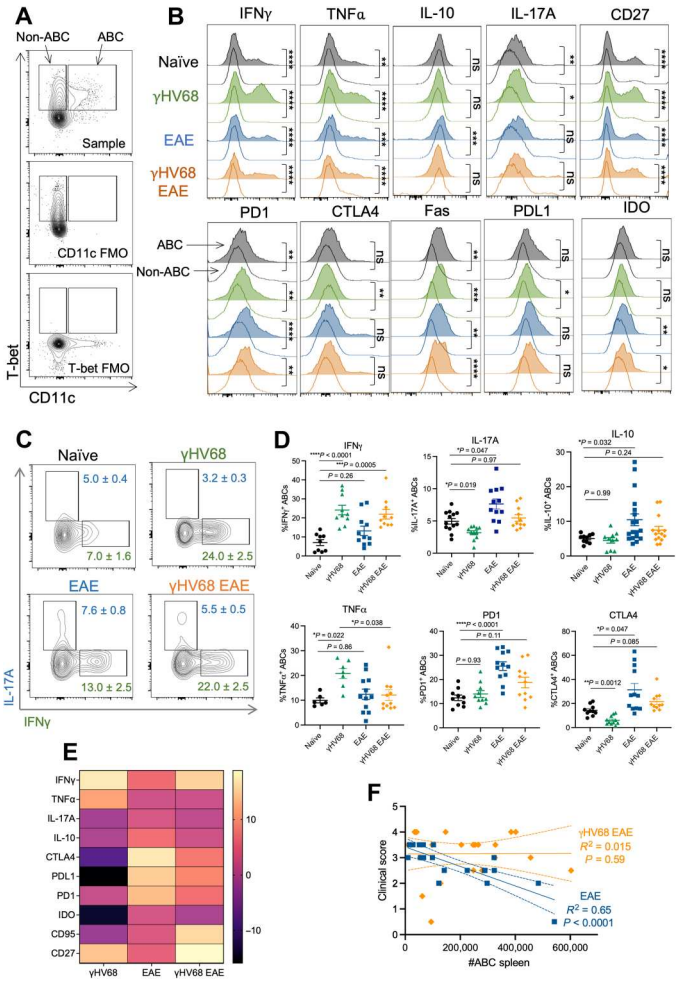

Fig. 2. γHV68 infection and EAE drive differential ABC phenotypes. Female C57BL/6(J) mice were mock-infected (naïve, black circles) or infected with γHV68 for 35 days (γHV68, green triangles). In some mice, $MOG_{35–55}$ EAE was induced 35 days after mock infection (EAE, blue squares) or γHV68 infection (γHV68 EAE, orange diamonds). At 35 days p.i. or 13 days after EAE induction, spleens were collected and processed for flow cytometry. (**A**) Flow plots of ABCs ($CD19^+CD11c^+$T-bet^+) and non-ABCs ($CD19^+CD11c^-$T-bet^+), previously gated on $CD19^+IgD^-$ live lymphocytes in the spleen. Representative sample alongside fluorescence-minus one (FMO) controls that lack either CD11c or T-bet staining. (**B**) Histogram plots of representative samples, previously gated on $CD19^+CD11c^+$T-bet^+ ABCs (area filled lines) or $CD19^+CD11c^-$T-bet^+ non-ABCs (empty lines) in the spleen, showing the modal expression of various markers. (**C**) Representative flow plots of expression of IFNγ and IL-17A on $CD19^+CD11c^+$T-bet^+ ABCs in the spleen. Files were concatenated from samples from the same treatment group. (**D**) Percent of splenic ABCs ($CD19^+CD11c^+$T-bet^+) that are positive for IFNγ, IL-17A, IL-10, TNFα, PD1, and CTLA4. (**E**) Heatmap representing changes in the frequency of the ABC population expressing given markers compared relative to naïve controls. (**F**) Linear regression of clinical scores versus number of splenic ABCs. Data are pooled across two to three experiments; n = 9 to 18 mice per group. Data are presented as means ± SD (C) or SEM (D), analyzed by Mann-Whitney test (B), one-way ANOVA with multiple comparisons (D), and simple linear regression with slope and 95% confidence interval plotted (F); $^{****}P < 0.0001$, $^{***}P < 0.001$, $^{**}P < 0.01$, and $^{*}P < 0.05$.

10 and inhibitory receptors, that is dampened in the presence of latent γHV68 infection, as ABCs in γHV68-EAE mice did not display the same increases in IL-10, PD1, or CTLA4 compared to naïve mice that are observed in EAE mice (Fig. 2, D and E). Analysis of a subset of extracellular markers demonstrates that a similar ABC phenotype is maintained between the brain and the spleen during EAE and γHV68-EAE (fig. S3). Insufficient numbers of ABCs precluded analysis of phenotypic markers in the spinal cord and CLNs.

Next, we analyzed the relationship between the number of ABCs in the spleen and the clinical disease score in EAE and γHV68-EAE mice. We observed that the number of ABCs in EAE mice negatively correlates with end point clinical score (Fig. 2F), indicating that ABCs might be contributing in a protective manner to disease. Alternately, there was no relationship between the number of ABCs and clinical score in γHV68-EAE mice (Fig. 2F). Therefore, we predict that ABCs are more pathogenic during γHV68-EAE compared to EAE. Together, these results highlight that γHV68 infection and EAE induction drive ABCs to take on unique phenotypes.

ABC functional capacities differ during γHV68 infection and EAE

ABCs are known to display functional capacities in addition to the secretion of cytokines, including the production of antiviral antibodies or autoantibodies and interactions with T cells. To investigate the functional capacities of ABCs during γHV68 infection and EAE, we used mice with a B cell–specific T-bet deletion (*14*) that lack ABCs. Female $Tbx21^{fl/fl}Cd19^{+/+}$ (Ctrl) and $Tbx21^{fl/fl}Cd19^{cre/+}$ [knockout (KO)] mice were mock-infected or infected with γHV68 for 35 days and induced for $MOG_{35–55}$ EAE. We observed a significant loss of ABCs in KO compared to Ctrl littermate controls (Fig. 3A and fig. S4A) and confirmed that T-bet deficiency in B cells does not alter the proportions of additional B cell subsets apart from ABCs, including germinal center B cells, plasmablasts, and non–class-switched B cells (fig. S4, B to D).

ABCs are major producers of antiviral antibodies and autoantibodies and are largely class-switched to IgG2a/c (*2*, *14*, *52*, *53*). To investigate ABC production of antibody during γHV68 infection and EAE, we analyzed the sera from mice with or without ABCs for IgG2c antibodies specific to γHV68 and $MOG_{35–55}$. We observed that the anti-γHV68 IgG2c titer in KO mice is significantly decreased compared to Ctrl mice in both γHV68 and γHV68-EAE mice (Fig. 3B). These results are in accordance with previous findings that report a loss of virus-specific antibody in the absence of ABCs (*2*, *52*, *54*). We then examined anti-$MOG_{35–55}$ IgG2c titers and, unexpectedly, did not observe differences between Ctrl and KO mice during EAE and γHV68-EAE (Fig. 3C). These results indicate that while ABCs are major producers of antiviral antibodies in the context of latent γHV68 infection, they do not contribute substantially to the anti-$MOG_{35–55}$ antibody response during EAE.

We speculated that ABCs could affect disease via skewing of T cell responses during autoimmunity, so we next examined the proportion of T cells and their expression of cytokines in the spleens of Ctrl and KO EAE and γHV68-EAE mice. We observed no difference in the proportions of CD8 or CD4 T cells in the spleen between Ctrl and KO mice during EAE or γHV68-EAE (fig. S5, A and B). Regulatory T cells displayed an increasing trend in KO mice in both EAE and γHV68-EAE mice, indicating that ABCs may dampen the regulatory T cell population during autoimmunity (Fig. 3D). To examine the skewing of peripheral T cells, we

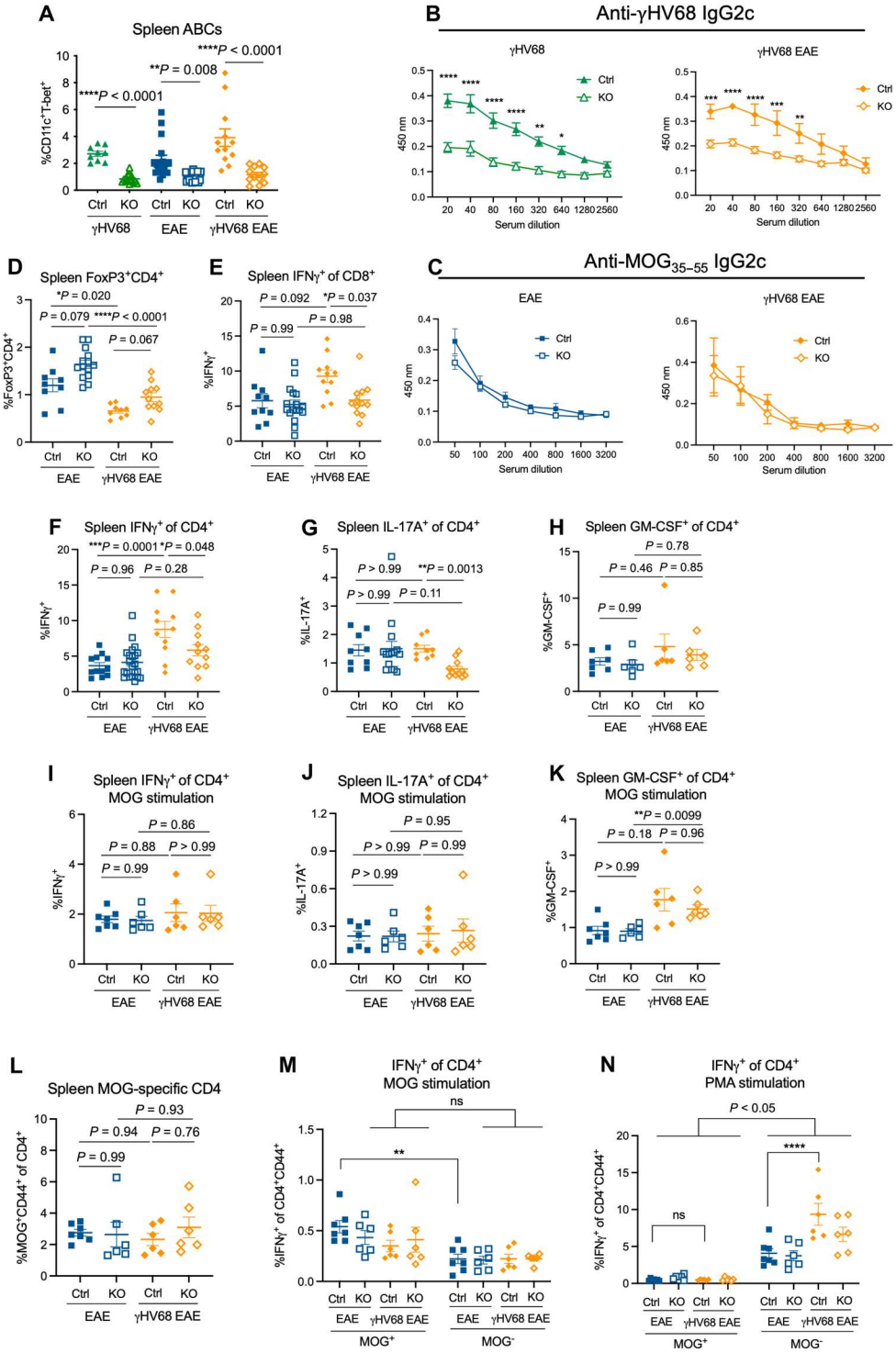

Fig. 3. ABC KO mice demonstrate different functional capacities during EAE and γHV68 infection. Female *Tbx21*$^{fl/fl}$*Cd19*$^{cre/+}$ (KO, open symbols) and *Tbx21*$^{fl/fl}$*Cd19*$^{+/+}$ (Ctrl, filled symbols) mice were infected with γHV68 or mock-infected for 35 days and then induced for $MOG_{35–55}$ EAE. At days 13 to 18 after EAE induction, blood, spleens, brains, and spinal cords were collected. Spleens, brains, and spinal cords were processed for flow cytometry, and serum was collected from blood. (**A**) Percent ABCs ($CD11c^+$T-bet^+) of previously activated B cells ($CD19^+IgD^-$) in the spleen of Ctrl and KO mice (n = 3 to 7 per group). (**B** and **C**) Optical density (y axis) reflecting titers (x axis; dilution of serum) of anti-$MOG_{35–55}$ (B) or anti-γHV68 (C) IgG2c antibodies in Ctrl and KO mice, separated by EAE and γHV68 EAE mice; n = 3 to 6 mice per group. (**D**) Percent of live cells in the spleen that are $CD4^+FoxP3^+$. (**E** to **H**) Splenocytes from Ctrl and KO mice stimulated with PMA/ionomycin. Percent $IFN\gamma^+$ of $CD3^+CD8^+$ (E) and $CD3^+CD4^+$ (F), and percent $CD4^+$ T cells expressing IL-17A (G) and GM-CSF (H) are reported. (**I** to **K**) Splenocytes from Ctrl and KO mice stimulated with $MOG_{35–55}$ peptide. Percent $CD4^+$ T cells expressing IFNγ (I), IL-17A (J), or GM-CSF (K) following MOG stimulation. (**L**) Proportion of $CD44^+$ MOG-specific $CD4^+$ T cells in the spleen of Ctrl and KO mice. (**M** and **N**) Splenocytes from Ctrl and KO mice stimulated with MOG peptide (M) or PMA (N) and the proportion of $CD4^{+-}$ $CD44^+MOG^+$ or $CD4^+CD44^+MOG^-$ cells expressing IFNγ. Data are presented as means ± SEM. Analyzed by Mann-Whitney test (A), two-way ANOVA (B, C, M, and N), or one-way ANOVA with multiple comparisons (D to L); ****P < 0.0001, ***P < 0.001, **P < 0.01, and *P < 0.05.

stimulated splenocytes with phorbol 12-myristate 13-acetate (PMA)/ionomycin and examined the expression of IFNγ, IL-17A, and GM-CSF by flow cytometry. We observed that skewing of T cells is altered in KO mice during γHV68-EAE. Ctrl mice display increased IFNγ-expressing CD8 and CD4 T cells in the spleen in γHV68-EAE compared to EAE; however, this increase is not observed in KO mice (Fig. 3, E and F). In addition, significantly fewer CD4 T cells express IL-17A in KO mice during γHV68-EAE compared to Ctrl mice (Fig. 3G). No differences in the proportion of CD4 T cells expressing GM-CSF were observed between any of the groups (Fig. 3H). In contrast to γHV68-EAE mice, there were no changes in splenic T cell skewing during EAE between Ctrl and KO mice (Fig. 3, E to H, and fig. S5C). The decrease in proportions of T cells expressing IFNγ and IL-17A in KO mice during γHV68-

EAE likely indicates that, without ABCs, the peripheral immune response might shift away from a pathogenic state. These results indicate that ABCs affect T cell skewing in the spleen during γHV68-EAE, though not during EAE.

To better understand the specificity of the T cell response during autoimmunity, we stimulated splenocytes with MOG peptide to compare the MOG-specific and nonspecific response. We observed that the increased expression of IFNγ on CD4 T cells during γHV68-EAE in Ctrl mice observed following PMA stimulation was not present under the MOG-stimulated conditions (Fig. 3, I and J). In addition, the decrease in IFNγ and IL-17A expression on CD4 T cells in KO γHV68-EAE mice compared to Ctrl was not observed under the MOG-stimulated conditions (Fig. 3, I and J). These data indicate that ABCs do not drive IFNγ expression of MOG-specific T cells but do affect its expression in non–MOG-specific T cells, some of which are likely γHV68 specific. Intriguingly, we observed an increase in GM-CSF expression by CD4 T cells in KO γHV68-EAE compared to KO EAE mice with MOG stimulation (Fig. 3K), which was not observed under the PMA-stimulated conditions (Fig. 3H), which highlights the possibility that GM-CSF production by CD4 T cells is a MOG-specific response that is affected by infection. As expression is unchanged between Ctrl and KO mice during EAE or γHV68-EAE (Fig. 3, H and K), it appears that GM-CSF expression by CD4 T cells is not dictated by the presence of ABCs.

Next, we examined MOG-specific CD44$^+$ CD4 T cells by stimulating splenocytes ex vivo with MOG (fig. S5D), as ABCs have previously been shown to be capable antigen presenters (*5*). We observed no difference in the proportion of MOG-specific CD44$^+$ CD4 T cells between Ctrl and KO mice during EAE or γHV68-EAE (Fig. 3L). This finding indicates that, in the context EAE, ABCs do not appear to be acting as $MOG_{35–55}$ APCs. We have also previously shown no difference in CD8 T cells specific to γHV68 during latent infection between Ctrl and KO mice (*55*).

We then examined the production of IFNγ by MOG tetramer–positive versus MOG tetramer–negative CD4 T cells in Ctrl and KO mice during EAE and γHV68-EAE. Following stimulation with $MOG_{35–55}$, activated MOG tetramer–positive cells express comparable or elevated levels of IFNγ than activated MOG tetramer–negative CD4 T cells during EAE and γHV68-EAE (Fig. 3M). However, when stimulated nonspecifically with PMA, MOG tetramer–negative CD4 T cells express more IFNγ than MOG-specific CD4 T cells under all conditions (Fig. 3N). MOG tetramer–negative cells from γHV68-EAE mice express significantly more IFNγ than those from mice with EAE only (Fig. 3N). This increase in IFNγ is not maintained in the MOG tetramer–positive population (Fig. 3N). These data suggest that the overall increase in IFNγ production by CD4 T cells in γHV68-EAE (Fig. 3F) is due to cells that are not MOG specific but, rather, are likely specific to γHV68.

Together, these findings highlight the heterogeneity of the ABC response to virus versus self-peptide antigen. ABCs produce anti-γHV68 antibodies but are not major producers of anti-MOG antibodies. In addition, these results indicate that ABCs do not appear

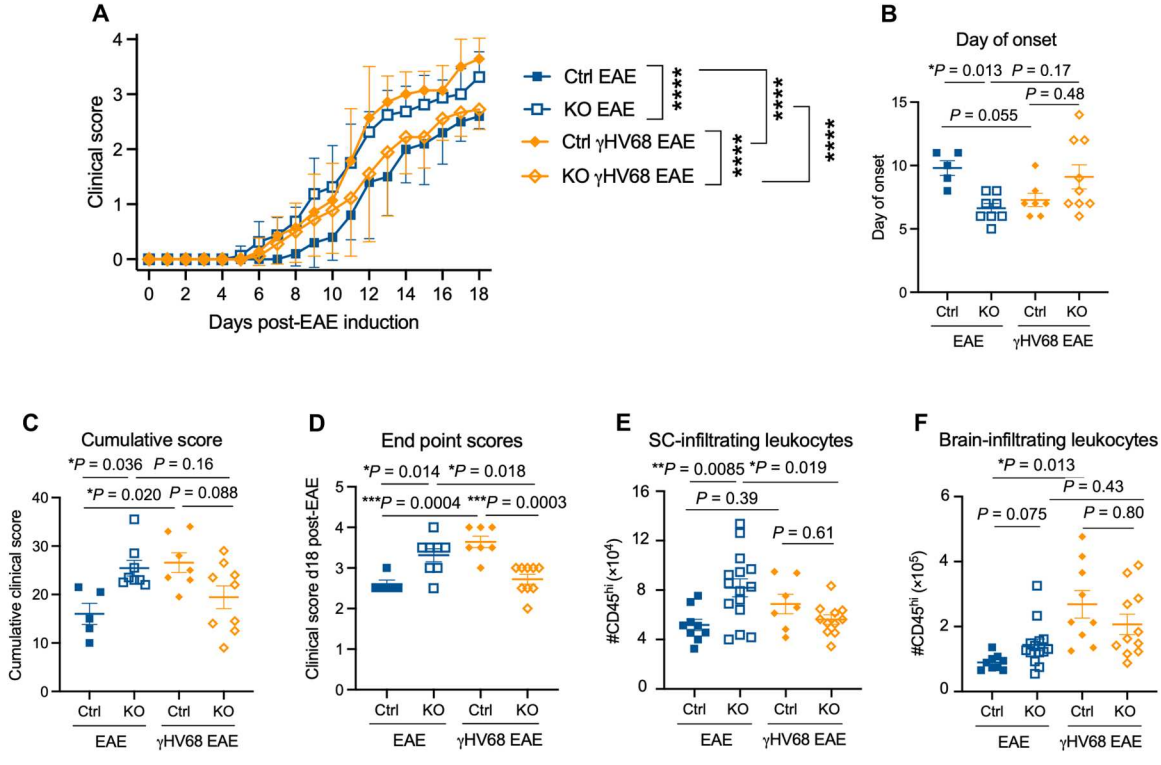

Fig. 4. EAE disease course is altered in ABC KO mice. Female *Tbx21*$^{fl/fl}$*Cd19*$^{cre/+}$ (KO, open symbols) and *Tbx21*$^{fl/fl}$*Cd19*$^{+/+}$ (Ctrl, filled symbols) mice were infected with γHV68 or mock-infected for 35 days and then induced for $MOG_{35–55}$ EAE and clinically monitored for 18 days. (**A**) EAE clinical scores; $n = 5$ to 9 per group. (**B**) Day of clinical symptom onset after induction. (**C**) Cumulative scores and (**D**) end point scores at day 18 after EAE induction. (**E** and **F**) Number of CD45^{hi} cells in the spinal cord (E) and brain (F). Data were analyzed by (A) two-way ANOVA with multiple comparisons or (B to F) one-way ANOVA with multiple comparisons. Data are pooled across three independent experiments, presented as means ± SD (A) or means ± SEM (B to F); ****$P < 0.0001$, ***$P < 0.001$, **$P < 0.01$, and *$P < 0.05$.

to influence MOG-specific T cells, although ABCs do dictate IFNγ and IL-17A expression on non–MOG-specific CD4 T cells. These results demonstrate that ABCs take on not only different phenotypes but also functional capacities during γHV68 infection and EAE.

ABCs are protective in EAE and pathogenic in γHV68-EAE

Next, we sought to determine whether ABCs contribute to the EAE or γHV68-EAE clinical disease course. Previously, our laboratory has shown that latent γHV68 infection before disease induction results in an exacerbated clinical course, with a T_H1 skewed immune response and increased CD8 T cell infiltration to the CNS (*48*). To investigate the role of ABCs in disease, we induced EAE, with or without latent γHV68 infection, in ABC KO and Ctrl mice, and examined the clinical course. Mice were monitored daily after EAE induction, blinded to genotype, and measured on a five-point scale as previously described (*48*). Notably, we observed that $MOG_{35–55}$ EAE induction of mice lacking ABCs had the opposite effect on the clinical course in EAE and γHV68-EAE. Specifically, during EAE, KO mice developed more severe disease than Ctrl mice, while in γHV68-EAE, the disease course was less severe than Ctrl mice (Fig. 4A). During EAE, KO mice displayed an earlier day of onset and higher cumulative and end point scores than Ctrl mice (Fig. 4, B to D). In contrast, γHV68-EAE KO mice displayed a lower end point score (Fig. 4D). These results indicate that ABCs contribute protectively in EAE and pathogenically in γHV68-EAE and align with our previous observations that ABCs display a more pathogenic phenotype in γHV68-EAE compared to EAE. In addition, while Ctrl γHV68-EAE mice displayed an exacerbated disease course compared to EAE alone, KO mice did not display exacerbation, thereby demonstrating that ABCs are required for γHV68-mediated enhancement of EAE.

In EAE mice, we observed significant differences in CNS leukocyte infiltration. KO mice induced for EAE displayed increased numbers of leukocytes infiltrating the spinal cord, where disease predominates, compared to Ctrl (Fig. 4E). This indicates that ABCs in EAE mice could possibly be influencing CNS leukocyte homing or blood-brain barrier integrity (Fig. 4, E and F). There was no significant difference in abundance of CNS-infiltrating leukocytes in γHV68-EAE, indicating that ABCs are influencing disease through a different mechanism. ABC deficiency did not result in significant differences in the numbers of CD8, CD4, or regulatory T cells infiltrating the CNS during EAE or γHV68-EAE (fig. S6, A to F). These results require further analysis to understand the cell populations that are infiltrating the CNS in KO mice during EAE.

Previous work has shown that specifically deleting T-bet from B cells leads to an inability of mice to control chronic LCMV infection (*2*, *52*). To test the impact of knocking out ABCs on viral load, we performed quantitative polymerase chain reaction analysis and observed an increased quantity of γHV68 in the spleens of KO mice compared to Ctrl during γHV68-EAE (fig. S6G). The ability of ABCs to control γHV68 infection and the impact on the clinical course of disease warrants further investigation.

Together, these findings demonstrate that ABCs opposingly influence EAE and γHV68-EAE disease course, thus indicating that ABCs contribute protectively to EAE and pathogenically to γHV68-EAE. The precise mechanisms by which ABCs affect T cell skewing and lymphocyte migration to and infiltration of the CNS warrant further investigation.

EBV serostatus and relapsing MS diagnosis alter the circulating ABC population

To confirm translatability of in vivo findings to people with MS, we compared the ABC population frequency and phenotype in individuals with and without a history of EBV infection and relapse-remitting MS (RRMS). Peripheral blood mononuclear cells (PBMCs) were collected from EBV^- and EBV^+ healthy females as well as female donors with RRMS, all of whom were EBV^+, and the ABC proportion and phenotype were examined by flow cytometry. The people diagnosed with RRMS were not exposed to immunomodulatory treatments and had disease durations ranging from 4 months to 7 years (Table 1). Median ages between groups were comparable:

Table 1. Donor disease characteristics and serology. HD, healthy donor; EDSS, Expanded Disability Status Scale; VCA, viral capsid antigen; EBNA-1, Epstein-Barr nuclear antigen 1.

Donor ID	Age at donation (years)	Age (years) at MS symptom onset	EDSS score at time of donation	Disease duration at time of donation	EBV serostatus	CMV serostatus
MS-01	25	23	2.0	2 years 8 months	VCA^+ $EBNA\text{-}1^+$	–
MS-02	24	24	2.5	4 months	$VCA^+EBNA\text{-}1^+$	+
MS-03	31	31	2.5	6 months	VCA^+ $EBNA\text{-}1^-$	+
MS-04	32	26	2.0	5 years	VCA^+ $EBNA\text{-}1^+$	–
MS-05	39	31	2.0	7 years	VCA^+ $EBNA\text{-}1^+$	–
HD-01	25	N/A	N/A	N/A	VCA^- $EBNA\text{-}1^-$	–
HD-02	26	N/A	N/A	N/A	VCA^- $EBNA\text{-}1^-$	–
HD-03	18	N/A	N/A	N/A	VCA^- $EBNA\text{-}1^-$	+
HD-04	39	N/A	N/A	N/A	VCA^+ $EBNA\text{-}1^+$	–
HD-05	23	N/A	N/A	N/A	VCA^+ $EBNA\text{-}1^+$	+
HD-06	25	N/A	N/A	N/A	VCA^+ $EBNA\text{-}1^-$	+
HD-07	28	N/A	N/A	N/A	VCA^+ $EBNA\text{-}1^+$	–

EBV⁻ healthy donors (25 years ± 4.4), EBV⁺ healthy donors (26.5 years ± 7.1), and EBV⁺ people with RRMS (31 years ± 6.1; Table 1). Nearly 100% of MS patients are EBV seropositive (*29*, *30*, *34*), precluding analysis of EBV-seronegative MS donors.

For this study, human ABCs were defined as $CD19^{+}CD20^{+-}CD11c^{+}CD21^{-}$ (Fig. 5A). Gene analysis has shown that $CD19^{+}CD21^{-}$ B cells display high levels of CD11c and express T-bet (*7*, *56*). Furthermore, CD11c and CD21 have been used by other groups to define ABCs in people (*3*, *6*). Only extracellular staining was performed to preserve cell numbers due to the low abundance of ABCs in blood.

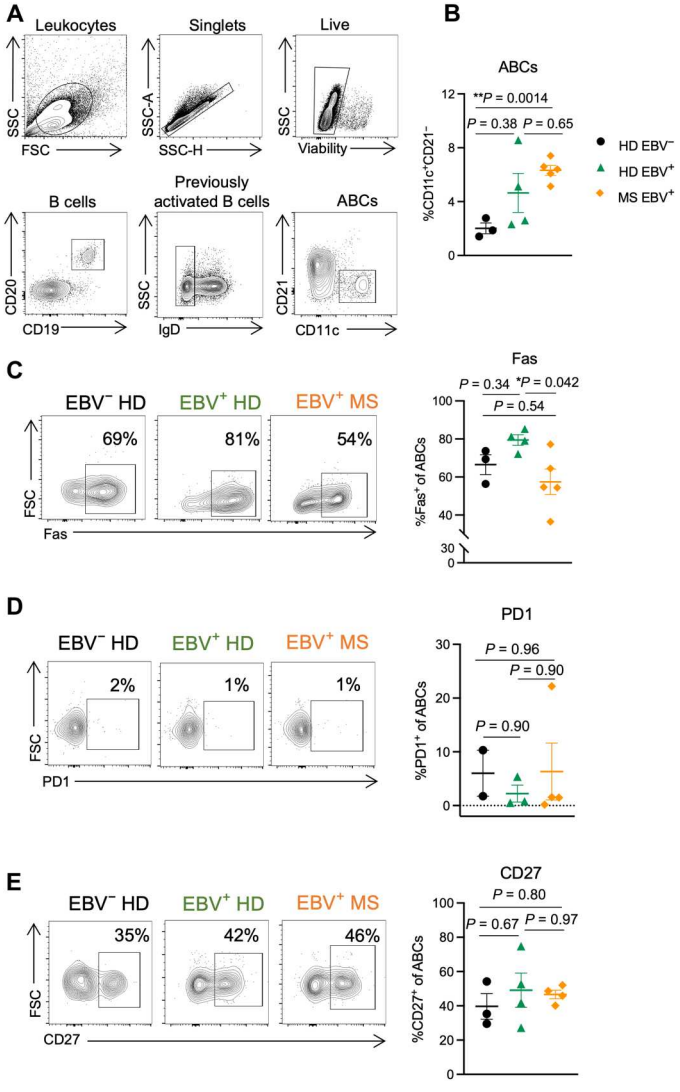

Fig. 5. The peripheral ABC phenotype is affected by EBV infection and MS status. PBMCs were collected from three EBV-seronegative healthy females (EBV⁻ HD, black circles), four EBV-seropositive healthy females (EBV⁺ HD, green triangles), and five females with RRMS that are all EBV seropositive (EBV⁺ MS, orange diamonds). PBMCs were processed for flow cytometry immediately following isolation. (**A**) Representative gating strategy for ABCs ($CD19^{+}CD20^{+}CD11c^{+}CD21^{-}$) from human PBMCs. (**B**) Proportion of ABCs ($CD11c^{+}CD21^{-}$) among previously activated B cells ($CD19^{+}CD20^{+}IgD^{-}$). (**C** to **E**) Representative samples and percent of ABCs ($CD19^{+}CD20^{+}CD11c^{+}CD21^{-}$) positive for (C) Fas, (D) PD1, and (E) CD27. Data for CD27- and PD1-stained samples are fewer ($n = 2$ to 4 donors per group) due to later addition of these markers following initial findings. Data are presented as means ± SEM, analyzed by one-way ANOVA with multiple comparisons; $^{**}P < 0.01$ and $^{*}P < 0.05$.

We found that people with RRMS have increased proportions of circulating ABCs compared to EBV-seronegative healthy people (Fig. 5B). EBV-seropositive healthy individuals show a nonsignificant trend toward increased ABC proportions compared to EBV-seronegative healthy people but reduced compared to RRMS (Fig. 5B). Among the donor groups, we do not observe differences in the proportion of total circulating B cells (fig. S7A). These findings indicate that both EBV infection and RRMS expand the proportion of circulating ABCs without significantly altering total B cell frequency. In addition to changes to ABC proportions, we also observe differences in ABC phenotype between groups.

Our preliminary analysis focused on the proportion of ABCs expressing Fas, PD1, and CD27. ABCs have previously been shown to express substantially more Fas than non-ABC B cells (*3*, *56*), and ABCs in people with common variable immune deficiency express more Fas than those in healthy donors (*9*). Another inhibitory receptor, PD1, has also been shown to be up-regulated on ABCs compared to other B cell subsets in both healthy individuals and those with SLE (*10*, *17*). The role of CD27, a marker of memory in human B cells, on ABCs is not well understood—ABCs have been reported to express high CD27 (*3*), although some groups define ABCs as CD27 negative (*17*, *56*). It is not known how infection versus autoimmunity affects the expression of Fas, PD1, and CD27 on ABCs. We observed that slightly over half of ABCs express Fas, and EBV infection led to a nonsignificant increase in the proportion of ABCs positive for Fas compared to EBV-seronegative healthy individuals (Fig. 5C). Among people who are EBV seropositive, RRMS led to a significant decrease in the proportion of ABCs expressing Fas compared to healthy donors (Fig. 5C). In contrast to previous reports (*10*, *17*), we found that a low proportion of ABCs express PD1 and the proportion of ABCs that express PD1 is not different across EBV-seronegative or EBV-seropositive healthy individuals or people with RRMS (Fig. 5D) Last, just under half of ABCs express CD27, and EBV and MS status did not affect the proportion of ABCs that express CD27 (Fig. 5E). Furthermore, we observed that cytomegalovirus (CMV) serostatus did not significantly correlate with the ABC phenotype in healthy individuals, nor those with RRMS (fig. S7), similar to a recent study in patients by Ascherio's research group (*34*), further indicating that CMV, another herpesvirus, may be less influential on this B cell population compared to EBV.

DISCUSSION

Here, we have shown that the ABC population is differentially affected by viral infection and autoimmunity, in both mice and humans. We sought to directly compare the ABC population in these two contexts and examine ABCs under conditions of combined latent viral infection and autoimmunity, as it relates to EBV infection in MS patients. In addition, we examined the functional contributions of ABCs, including cytokine and antibody production and influence on T cells, and identified them as a mediator between latent gammaherpesvirus infection and CNS autoimmune disease.

γHV68 infection and EAE induction each elicit divergent ABC cytokine profiles and phenotypes, with infection resulting in a T_H1-

like profile, while EAE induction results in a more regulatory phenotype with increased inhibitory receptor and IL-10 expression. One factor that might contribute to the observed differences is the use of adjuvant in the EAE induction regime, which likely results in the interaction of emerging ABCs with cognate T cells, potentially skewing the phenotype and functionality of newly formed ABCs. The impact of adjuvant on the development of ABCs, and the context in which ABCs likely develop during autoimmunity, deserves further investigation. In addition to phenotypic and cytokine differences, we have shown that ABCs produce antiviral antibodies but we do not observe differences in MOG-specific titers between mice with and without ABCs, and a lack of ABCs does not affect MOG-specific T cells, although non–MOG-specific T cells are skewed. These results demonstrate the divergent impact by ABCs depending on context. In addition, we found that ABCs in γHV68-EAE mice take on a phenotype with characteristics of both the viral infection and disease, demonstrating that ABCs are a heterogeneous population, particularly when challenged by multiple antigens. These findings have implications for studying the human ABC population that is undoubtedly affected by an array of pathogens and contexts.

Further highlighting the heterogeneity of ABCs, it appears that ABCs contribute differentially to autoimmunity depending on the model, as we observed that ABCs contribute to EAE in a protective manner, as knocking them out results in an exacerbation of disease, while in a model of SLE ABCs appear to be contributing pathogenically (*14*). Functional differences in ABCs between models are also observed. In SLE, knocking out ABCs results in a significant decrease in anti-chromatin IgG2a/c titers and dampening of kidney damage and mortality (*14*). Alternatively, we do not observe differences in anti-MOG IgG2c antibody titers in the absence of ABCs. The mechanisms by which ABCs protect from severe EAE disease is not clear, although IL-10 production by B cells is known to contribute to EAE severity (*57*), and our results show elevated IL-10 expression on ABCs compared to non-ABCs, and its expression is particularly increased on ABCs during EAE. Critical to understanding the discrepancy in ABCs functioning protectively versus pathogenically in different models of autoimmune disease is further determining the mechanisms through which ABCs are affecting disease. We have previously reported that ABCs are required for γHV68 exacerbation of collagen-induced arthritis (*58*). The finding that ABCs are required for the γHV68 exacerbation of both collagen-induced arthritis (CIA) and EAE brings up the question of whether ABCs are a conserved mechanism by which gammaherpesvirus infection contributes to both RA and MS.

We observed that the ABC phenotype is differentially affected by viral infection and autoimmunity, although the phenotype observed in mice and humans does not exactly align. For instance, we observe that the proportion of ABCs that express Fas is decreased in people with RRMS compared to healthy EBV-positive donors, while in mice we observe an increase in γHV68-EAE compared with γHV68. This disconnect between the mouse and human ABC phenotype may be due to intrinsic differences between the immune systems in mice and humans or the lack of previous antigen exposure in the mice. In addition, it must be considered whether circulating ABCs are representative of those in the human spleen. We and others observed that ABCs are predominantly spleen-resident in mice (*18*), and further investigation should examine ABCs in the spleen versus circulation, especially as ABCs in people are primarily examined in blood.

A surprising finding of this study was the female sex bias of ABCs in the spleens of mice infected with γHV68 and/or induced for EAE. This finding is relevant to the question of whether ABCs play a role in the sex bias observed in various autoimmune diseases, including MS and SLE, as has previously been suggested (*59*). $MOG_{35–55}$ EAE does not display a sex bias in C57BL/6 mice (*50*, *51*), so whether and how the increased numbers of ABCs in female EAE mice affect disease in this model remains unknown.

Here, we have demonstrated that ABCs are required for the γHV68 exacerbation of EAE. In the absence of ABCs, the heightened clinical course observed in Ctrl γHV68 EAE mice is not observed. Our results demonstrate that ABCs play a pivotal role in controlling the peripheral T cell response, as the γHV68-induced T_H1 skewing during EAE is not observed in the absence of ABCs. However, the alterations to peripheral T cells between Ctrl and KO mice are not observed in the CNS during γHV68 EAE, and the local factors by which ABCs might influence disease within the CNS remain unclear. The increased γHV68 quantity in KO mice might indicate viral reactivation. Whether the virus is reactivating, and, if so, whether the presence of the lytic virus is modulating disease, deserves further examination. Recently, there has been increasing evidence for a role for antibodies that cross-react between EBV latency proteins and myelin proteins (*60*, *61*). In people, ABCs specific to EBV proteins could potentially cross-react with myelin proteins; ABCs persist long-term and undergo less somatic hypermutation than long-lived plasma cells (*20*, *62*), and thus could be more likely to react to multiple structurally similar antigens.

Our work, and that of others, demonstrates that ABCs are stimulated by an array of immune challenges, including viral infections, vaccinations, and autoimmunity (*2*, *6*, *13*, *17*, *18*, *21–23*, *52*, *53*, *63*, *64*). ABCs likely comprise several subsets that differ in terms of functional capacity, depending on the circumstances of the individual. In the future, it will be important to determine disease-associated subsets; a portion of ABCs could contribute to disease, and others may act in a regulatory/protective manner. An outstanding question is whether the ABC population is effectively depleted by disease-modifying therapies that remove some but not all B cells, such as rituximab, and whether the ABC population is affected by other immunomodulatory treatments. Depletion or modulation of ABCs might be a viable therapeutic opportunity to improve disease outcomes.

In summary, we have shown that (i) ABCs expand in the spleen in a sex-biased manner during γHV68 infection and EAE; (ii) ABCs display distinct phenotypes and functional capacities during γHV68 infection and EAE; (iii) knocking out ABCs results in exacerbation of EAE disease but, conversely, the loss of γHV68-mediated exacerbation of EAE; and (iv) EBV status and MS diagnosis affect the proportion of circulating ABCs and their phenotype in people. We hope that these findings can contribute to a better understanding of the ABC population and the relationship between EBV infection and MS.

MATERIALS AND METHODS

Mice

C57BL/6(J) mice were purchased from the Jackson Laboratory. $Tbx21^{fl/fl}Cd19^{cre/+}$ mice were generated by crossing $Tbx21^{fl/}$

$^{fl}Cd19^{cre/+}$ and $Tbx21^{fl/fl}Cd19^{+/+}$ mice with $Tbx21^{fl/fl}$ and $Cd19^{cre/+}$ mice provided by P. Marrack (*14*). All animals were bred and maintained in a specific pathogen–free animal facility at the University of British Columbia. Mice were housed in individually ventilated cages in groups of up to five animals per cage on corn cob bedding (Bed-o'Cobs, The Andersons) with unrestricted access to food (PicoLab Rodent Diet 20, #5053) and water on a 14.5- to 9.5-hour light-dark cycle. All animal work was approved by the Canadian Council for Animal Care (protocols A17-0105 and A17-0184) and performed in accordance with relevant guidelines and regulations, following recommendations in the ARRIVE guidelines.

γHV68 infection

γHV68 [WUMS strain, purchased from the American Type Culture Collection (ATCC) VR-1465] was propagated on baby hamster kidney (BHK-21, ATCC CCL-10) cells and quantified by plaque assay. Mice were infected with γHV68 or mock-infected with minimum essential medium (MEM; Gibco). For infection, virus was diluted in MEM and maintained sterile and on ice until infection. Six- to 10-week-old mice were intraperitoneally infected with 10^4 plaque-forming units of γHV68. No clinical symptoms were observed from viral infection.

Induction and evaluation of EAE

EAE was induced 35 days after γHV68 infection by injecting 100 μl of emulsified Complete Freund's Adjuvant (DIFCO) containing 200 μg of $MOG_{35–55}$ (GenScript) and 400 μg of desiccated *Mycobacterium tuberculosis* H37ra (DIFCO) subcutaneously. Mice also received two doses of 200 ng of pertussis toxin (List Biologicals) intraperitoneally at the time of immunization and 48 hours after induction. Mice were assessed daily (blinded) on a scale from 0 to 5: 0, no clinical symptoms; 0.5, partially limp tail; 1, paralyzed tail; 2, loss of coordination; 2.5, one hindlimb paralyzed; 3, both hindlimbs paralyzed; 3.5, both hindlimbs paralyzed accompanied by weakness in the forelimbs; 4, forelimbs paralyzed (humane end point); 5, moribund or dead. Onset is defined as two consecutive days of a score of 0.5 or above. Supportive care provided included administration of subcutaneous fluids and provision of nutritional gel.

Tissue collection and processing

Mice were euthanized by cardiac puncture while anesthetized with isoflurane and immediately perfused with 20 cm^3 of phosphate-buffered saline (PBS) to allow for brain and spinal cord harvesting without blood contamination. Spleen, brain, spinal cord, and CLNs were extracted, placed into PBS, and temporarily kept on ice until processing. Spleens, spinal cords, and CLNs were mashed through a 70-μm cell strainer, and a single-cell suspension was prepared for each sample. Brains were mashed through a 70-μm cell strainer twice, and a single-cell suspension was prepared for each sample. Splenocytes were incubated in ammonium-chloride-potassium (ACK) lysing buffer for 10 min on ice to lyse red blood cells, and the remaining cells were kept on ice until further use. Immune cells were isolated from brains and spinal cords using a 30% Percoll gradient (GE Healthcare) and were resuspended in flow cytometry staining buffer [fluorescence-activated cell sorting (FACS) buffer, PBS with 2% newborn calf serum; Sigma-Aldrich] until staining.

Flow cytometric analysis of cell type–specific surface antigens and intracellular cytokines

To evaluate cytokine production by various cell types, 4 million splenocytes were stimulated ex vivo for 3 hours at 5% CO_2 at 37°C in MEM (Gibco) containing 10% fetal bovine serum (FBS; Sigma-Aldrich), GolgiPlug (1 μl/ml; BD Biosciences), PMA (10 ng/ml; Sigma-Aldrich), and ionomycin (500 ng/ml; Thermo Fisher Scientific). Alternatively, cells were stimulated ex vivo for 5 hours at 5% CO_2 at 37°C in MEM containing 10% FBS, with $MOG_{35–55}$ (50 μg/ml) and GolgiPlug (1 μl/ml). Stimulated cells were then washed before staining. For each spleen sample, 4 million cells were stained in two wells of a 96-well plate, with 2 million cells per well. All collected brain and spinal cord cells were resuspended in FACS buffer and stained in a single well. Blood donor PBMC samples were stained at 1 million cells per well using the following method without ex vivo stimulation. Before staining, samples were incubated for 30 min at 4°C with Fixable Viability Dye eFluor506 (2 μl/ml; Thermo Fisher Scientific) while in PBS. Cells were then incubated with a rat anti-mouse CD16/32 (Fc Block, BD Biosciences) antibody or Human BD Fc Block (BD Biosciences) for 10 min at room temperature (RT). For tetramer staining, cells were incubated in phycoerythrin (PE)–conjugated MOG:I-A^b (6.5 μg/ml; $MOG_{38–49}$: GWYRSPFSRVVH, NIH Tetramer Core Facility) covered for 1 hour at RT. Fluorochrome-labeled antibodies against cell surface antigens were then added to the cells for 30 min covered from light at 4°C. After washing, cells were resuspended in Fix/Perm buffer (Thermo Fisher Scientific) for 30 min to 12 hours covered from light at 4°C, washed twice with Perm buffer, and incubated for 40 min with antibodies against intracellular antigens in Perm buffer. Cells were then washed and resuspended in FACS buffer with 2 mM EDTA. Cells were stained with antibodies from Thermo Fisher Scientific, BioLegend, and BD Biosciences (Table 2). Samples were collected on Attune NxT Flow Cytometer (Thermo Fisher Scientific) or CytoFLEX LX N3-V5-B3-Y5-R3-I0 (BD Biosciences) and analyzed with FlowJo software version 10 (FlowJo LLC). Full-minus-one controls were used for gating.

Anti-$MOG_{35–55}$ and anti-γHV68 antibody ELISA

Serum was collected via cardiac puncture and maintained at RT to allow clotting. The sera were isolated by centrifugation at 2000*g* for 10 min, aliquoted, and stored for up to 6 months at −80°C before running the enzyme-linked immunosorbent assay (ELISA). Serum anti-$MOG_{35–55}$ and anti-γHV68 antibodies were quantified by standard indirect ELISA. Briefly, ELISA plates (NUNC, Thermo Fisher Scientific) were coated with antigen resuspended in coating buffer [0.05 M carbonate buffer (pH 9.6)] overnight at 4°C. For MOG ELISA, plates were coated with 1 μg of $MOG_{35–55}$ resuspended in coating buffer. For γHV68 ELISA, γHV68 virions were inactivated in 4% paraformaldehyde (PFA) for 20 min at RT. Then, plates were coated with γHV68 (5 μg/ml) in coating buffer with 1% PFA. The following day, plates were washed 4× with wash buffer (PBS and 0.05% Tween 20), blocked with 5% newborn calf serum (Sigma-Aldrich) for 1 hour at 37°C, incubated with serial dilutions (MOG: 1:50 to 1:3200; γHV68: 1:20 to 1:2560) of test sera diluted in blocking buffer for 2 hours at 37°C, and washed 4× with wash buffer. Bound antibody was incubated with horseradish peroxidase (HRP)–conjugated goat anti-mouse IgG2c (Thermo Fisher Scientific) diluted 1:500 in blocking buffer, for 1 hour at 37°C, washed

Table 2. Flow cytometry antibodies.

	Antigen	Fluorophore	Clone	Company
Anti-mouse antibodies	CD19	PE or FITC	ID3	Thermo Fisher Scientific
	CD11c	APC	N418	BioLegend
	CD11c	Alexa Fluor 700	N418	Thermo Fisher Scientific
	T-bet	PerCpCy5.5 or PE	4B10	Thermo Fisher Scientific
	IgD	PE-Cy7	11-26c	Thermo Fisher Scientific
	IFNγ	APC	XMG1.2	Thermo Fisher Scientific
	TNFα	PE-Cy7	MP6-Xt22	BioLegend
	IL-10	Pacific Blue	JES5-16E3	BioLegend
	IL-17A	PE-Dazzle594	TCII-18H10.1	BioLegend
	CTLA4	PE-Dazzle594	UC10-4B9	BioLegend
	PDL1	SB436	MIH5	Thermo Fisher Scientific
	PD1	SB436	J43	Thermo Fisher Scientific
	IDO	PerCpeFluor 710	mIDO-48	Thermo Fisher Scientific
	Fas	FITC	SA367H8	BioLegend
	CD27	PE-Cy7	LG.7F9	BioLegend
	CD45	PerCpCy5.5	30-F11	Thermo Fisher Scientific
	CD4	Alexa Fluor 700	RM4-5	Thermo Fisher Scientific
	CD8	APC-eFluor 780	53-6.7	Thermo Fisher Scientific
	FoxP3	FITC	FJK-16S	Thermo Fisher Scientific
	CD3e	eFluor 450	500A2	Thermo Fisher Scientific
	IL-6	eFluor 450	MP5-20F3	Thermo Fisher Scientific
	GM-CSF	PE-Cy7	MP1-22E9	Thermo Fisher Scientific
	BAFF	Biotin	IC9	Enzo
Anti-human antibodies	CD19	APC-eFluor 780	HIB19	Thermo Fisher Scientific
	IgD	FITC	IA6-2	BD Biosciences
	CD11c	Alexa Fluor 700	B-ly6	BD Biosciences
	CD21	PerCpCy5.5	Bu32	BioLegend
	CD20	Pacific Blue	2H7	BioLegend
	CD27	PE-Cy7	LG.3A1	BioLegend
	Fas	PE Texas Red	DX2	BD Biosciences
	PD1	PE	MIH4	Thermo Fisher Scientific

4× with wash buffer, and detected by trimethylboron (TMB) substrate addition (BD Biosciences). The plates were read at 450 nm on VarioSkan Plate Reader (Thermo Fisher Scientific) within 10 min of adding stop solution.

Donor recruitment and enrolment

Five individuals with relapsing MS were recruited at the Burnaby Hospital MS Clinic (Fraser Health) under the supervision of G. Vorobeychik. Seven unaffected donors were recruited at the Life Sciences Center (University of British Columbia). All donors were female, were 19 to 39 years of age (mean age, 28 ± 6.4 years), and provided written informed consent before enrolment in the study. Donors with a definite RRMS diagnosis, according to Poser or 2010 McDonald criteria, and disease duration of less than 10 years, were confirmed as treatment naïve before donation (no previous use of any disease-modifying therapies during lifetime). MS donors underwent a neurological exam the day of blood donation to assess Expanded Disability Status Scale (EDSS). Individuals with a progressive MS diagnosis or EDSS >4, who were male, pregnant, outside the designated age range, or undergoing treatment, were excluded from the present study.

Donor blood collection and processing

Blood samples were obtained by venipuncture and assigned an alphanumeric identifier. Whole blood was processed for PBMC isolation by Lymphoprep (StemCell) gradient separation, according to the manufacturer's instructions, within an hour of collection in K2-EDTA–coated vacutainer tubes (BD Biosciences). Freshly isolated

PBMCs were counted and stained for flow cytometric analysis (no previous freezing or other preservation steps used). Serum was obtained by centrifugation of untreated blood samples and frozen at −80°C for subsequent analysis.

Donor serology

Endogenous antibodies to EBV and CMV were detected using ELISAs to determine donor history of infection. Nunc Maxisorp 96-well microtiter ELISA plates (Thermo Fisher Scientific) were coated overnight at 4°C with 1 μg per well of the peptide of interest (Table 3) in carbonate buffer. For EBV EBNA-1 and CMV, epitope peptides 1 and 2 were mixed together before well coating. The following day, the plates were washed with PBS and wash buffer (PBS + 0.05% Tween 20), followed by a 2-hour blocking step at RT using wash buffer + 3% bovine serum albumin. Plates were washed again and then incubated with serum samples diluted in blocking buffer. Serum diluted 1:1000 was used to determine seropositivity to EBV and CMV antigens. After a 2-hour RT incubation with serum, the plates were washed and then incubated with HRP-labeled goat anti-human IgG antibody (Thermo Fisher Scientific) diluted 1:3000 in blocking buffer or HRP-labeled goat anti-human IgM (Thermo Fisher Scientific) diluted 1:4000 at 37°C for 1 hour. The plates were then washed with PBS before the addition of TMB substrate (100 μl per well; BD Biosciences). Fifteen minutes after the addition of substrate, 100 μl of stop solution (2 M sulfuric acid) was added to each well. The plates were read at 450 nm on VarioSkan Plate Reader (Thermo Fisher Scientific) within 10 min of adding stop solution.

Statistical analysis

Data and statistical analyses were performed using GraphPad Prism software 8.4.2 (GraphPad Software Inc.). Results are presented as means ± SEM or means ± SD. Number of mice per group (n), statistical significance (P value), and the number of experimental replicates are indicated in the figure legends. For comparison of two groups, a Mann-Whitney test was used. Comparison of three or more groups was done by one-way analysis of variance (ANOVA), with data that were not normally distributed analyzed by Kruskal-Wallis one-way ANOVA. Correlation between clinical score and number of ABCs was determined by simple linear regression. For group comparisons with two variables, such as ELISA absorbance values and serum dilutions, an ordinary two-way ANOVA was used. When more than two groups were present, such as clinical EAE scores over time, a two-way ANOVA with Tukey's multiple comparisons test was used, and the main column effect was reported. Data points were omitted from data analysis due to attrition. P values are indicated by asterisks as follows: $^{****}P < 0.0001$, $^{***}P < 0.001$, $^{**}P < 0.01$, and $^{*}P < 0.05$.

Table 3. Donor serology peptide sequences.

Antigen	Peptide sequence
EBV VCA p18	ASAGTGALASSAPSTAVAQSATPSVSSSISSLRAATSGA TAAAAVDTGS GGGGQPHDTAPRGARKKQ
EBV EBNA-1	Epitope 1: RSPSSQSSSSGSPPRRPPPGRRPFFHPVG
	Epitope 2: DYFEYHQEGGPDGEPDVPPGAIEQGPADDPG EGPSTGPRG
CMV	Epitope 1: CETDDLDEEDTSIYLSPPPVPPVQVVAKRLPRP DTPRT
	Epitope 2: KSGTGPQPGSAGMGGAKTPSDAVQNILQKIE KIKNTEE

Study approval

Animal work was approved by the Animal Care Committee of the University of British Columbia (protocols A17-0105 and A17-0184). The human blood donation protocol (H16-02338) was approved by the University of British Columbia Clinical Research Ethics Board and by the Fraser Health Authority.

Supplementary Materials

This PDF file includes:

Supplementary Methods: γHV68 quantitation
Tables S1 and S2
Figs. S1 to S7

View/request a protocol for this paper from *Bio-protocol*.

REFERENCES AND NOTES

1. Y. Hao, P. O'Neill, M. S. Naradikian, J. L. Scholz, M. P. Cancro, A B-cell subset uniquely responsive to innate stimuli accumulates in aged mice. *Blood* **118**, 1294–1304 (2011).
2. K. Rubtsova, A. V. Rubtsov, L. F. van Dyk, J. W. Kappler, P. Marrack, T-box transcription factor T-bet, a key player in a unique type of B-cell activation essential for effective viral clearance. *Proc. Natl. Acad. Sci. U.S.A.* **110**, E3216–E3224 (2013).
3. A. V. Rubtsov, K. Rubtsova, A. Fischer, R. T. Meehan, J. Z. Gillis, J. W. Kappler, P. Marrack, Toll-like receptor 7 (TLR7)-driven accumulation of a novel CD11c^{+} B-cell population is important for the development of autoimmunity. *Blood* **118**, 1305–1315 (2011).
4. M. Ratliff, S. Alter, D. Frasca, B. B. Blomberg, R. L. Riley, In senescence, age-associated B cells secrete TNFα and inhibit survival of B-cell precursors. *Aging Cell* **12**, 303–311 (2013).
5. A. V. Rubtsov, K. Rubtsova, J. W. Kappler, J. Jacobelli, R. S. Friedman, P. Marrack, CD11c-expressing B cells are located at the T cell/B cell border in spleen and are potent APCs. *J. Immunol.* **195**, 71–79 (2015).
6. N. Claes, J. Fraussen, M. Vanheusden, N. Hellings, P. Stinissen, B. Van Wijmeersch, R. Hupperts, V. Somers, Age-associated B cells with proinflammatory characteristics are expanded in a proportion of multiple sclerosis patients. *J. Immunol.* **197**, 4576–4583 (2016).
7. I. Isnardi, Y.-S. Ng, L. Menard, G. Meyers, D. Saadoun, I. Srdanovic, J. Samuels, J. Berman, J. H. Buckner, C. Cunningham-Rundles, E. Meffre, Complement receptor 2/CD21^{-} human naive B cells contain mostly autoreactive unresponsive clones. *Blood* **115**, 5026–5036 (2010).
8. C. Wehr, H. Eibel, M. Masilamani, H. Illges, M. Schlesier, H.-H. Peter, K. Warnatz, A new CD21low B cell population in the peripheral blood of patients with SLE. *Clin. Immunol.* **113**, 161–171 (2004).
9. M. Rakhmanov, B. Keller, S. Gutenberger, C. Foerster, M. Hoenig, G. Driessen, M. van der Burg, J. J. van Dongen, E. Wiech, M. Visentini, I. Quinti, A. Prasse, N. Voelxen, U. Salzer, S. Goldacker, P. Fisch, H. Eibel, K. Schwarz, H.-H. Peter, K. Warnatz, Circulating CD21low B cells in common variable immunodeficiency resemble tissue homing, innate-like B cells. *Proc. Natl. Acad. Sci. U.S.A.* **106**, 13451–13456 (2009).
10. S. Wang, J. Wang, V. Kumar, J. L. Karnell, B. Naiman, P. S. Gross, S. Rahman, K. Zerrouki, R. Hanna, C. Morehouse, N. Holoweckyj, H. Liu, Z. Manna, R. Goldbach-Mansky, S. Hasni, R. Siegel, M. Sanjuan, K. Streicher, M. P. Cancro, R. Kolbeck, R. Ettinger, IL-21 drives expansion and plasma cell differentiation of autoreactive CD11c^{hi}T-bet^{+} B cells in SLE. *Nat. Commun.* **9**, 1758 (2018).
11. L. Couloume, J. Ferrant, S. Le Gallou, M. Mandon, R. Jean, N. Bescher, H. Zephir, G. Edan, E. Thouvenot, A. Ruet, M. Debouverie, K. Tarte, P. Amé, M. Roussel, L. Michel, Mass cytometry identifies expansion of T-bet+ B cells and CD206+ monocytes in early multiple sclerosis. *Front. Immunol.* **12**, 653577 (2021).
12. K. Thorarinsdottir, A. Camponeschi, C. Jonsson, K. Granhagen Önnheim, J. Nilsson, K. Forslind, M. Visentini, L. Jacobsson, I.-L. Mårtensson, I. Gjertsson, CD21$^{-/low}$ B cells associate with joint damage in rheumatoid arthritis patients. *Scand. J. Immunol.* **90**, e12792 (2019).
13. I. C. Mouat, E. Goldberg, M. S. Horwitz, Age-associated B cells in autoimmune diseases. *Cell. Mol. Life Sci.* **79**, 402 (2022).

14. K. Rubtsova, A. V. Rubtsov, J. M. Thurman, J. M. Mennona, J. W. Kappler, P. Marrack, B cells expressing the transcription factor T-bet drive lupus-like autoimmunity. *J. Clin. Invest.* **127**, 1392–1404 (2017).
15. K. Rubtsova, A. V. Rubtsov, M. P. Cancro, P. Marrack, Age-associated B cells: A T-bet dependent effector with roles in protective and pathogenic immunity. *J. Immunol.* **195**, 1933–1937 (2015).
16. K. Rubtsova, A. V. Rubtsov, K. Halemano, S. X. Li, J. W. Kappler, M. L. Santiago, P. Marrack, T cell production of IFNγ in response to TLR7/IL-12 stimulates optimal B cell responses to viruses. *PLOS ONE* **11**, e0166322 (2016).
17. J. J. Knox, M. Buggert, L. Kardava, K. E. Seaton, M. A. Eller, D. H. Canaday, M. L. Robb, M. A. Ostrowski, S. G. Deeks, M. K. Slifka, G. D. Tomaras, S. Moir, M. A. Moody, M. R. Betts, T-bet+ B cells are induced by human viral infections and dominate the HIV gp140 response. *JCI Insight* **2**, e92943 (2017).
18. J. L. Johnson, R. L. Rosenthal, J. J. Knox, A. Myles, M. S. Naradikian, J. Madej, M. Kostiv, A. M. Rosenfeld, W. Meng, S. R. Christensen, S. E. Hensley, J. Yewdell, D. H. Canaday, J. Zhu, A. B. McDermott, Y. Dori, M. Itkin, E. J. Wherry, N. Pardi, D. Weissman, A. Naji, E. T. L. Prak, M. R. Betts, M. P. Cancro, The transcription factor T-bet resolves memory B cell subsets with distinct tissue distributions and antibody specificities in mice and humans. *Immunity* **52**, 842–855.e6 (2020).
19. A. Nellore, E. Zumaquero, C. D. Scharer, R. G. King, C. M. Tipton, C. F. Fucile, T. Mi, B. Mousseau, J. E. Bradley, F. Zhou, P. A. Goepfert, J. M. Boss, T. D. Randall, I. Sanz, A. F. Rosenberg, F. E. Lund, Influenza-specific effector memory B cells predict long-lived antibody responses to vaccination in humans. bioRxiv 643973 [Preprint]. 18 February 2021. https://doi.org/10.1101/643973.
20. J. W. Austin, C. M. Buckner, L. Kardava, W. Wang, X. Zhang, V. A. Melson, R. G. Swanson, A. J. Martins, J. Q. Zhou, K. B. Hoehn, J. N. Fisk, Y. Dimopoulos, A. Chassiakos, S. O'Dell, M. G. Smelkinson, C. A. Seamon, R. W. Kwan, M. C. Sneller, S. Pittaluga, N. A. Doria-Rose, A. McDermott, Y. Li, T.-W. Chun, S. H. Kleinstein, J. S. Tsang, C. Petrovas, S. Moir, Overexpression of T-bet in HIV infection is associated with accumulation of B cells outside germinal centers and poor affinity maturation. *Sci. Transl. Med.* **11**, eaax0904 (2019).
21. L.-Y. Chang, Y. Li, D. E. Kaplan, Hepatitis C viraemia reversibly maintains subset of antigen-specific T-bet+ tissue-like memory B cells. *J. Viral Hepat.* **24**, 389–396 (2017).
22. J. D. Eccles, R. B. Turner, N. A. Kirk, L. M. Muehling, L. Borish, J. W. Steinke, S. C. Payne, P. W. Wright, D. Thacker, S. J. Lahtinen, M. J. Lehtinen, P. W. Heymann, J. A. Woodfolk, T-bet+ memory B cells link to local cross-reactive IgG upon human rhinovirus infection. *Cell Rep.* **30**, 351–366.e7 (2020).
23. I. C. Mouat, M. S. Horwitz, Age-associated B cells in viral infection. *PLOS Pathog.* **18**, e1010297 (2022).
24. P. Holla, B. Dizon, A. A. Ambegaonkar, N. Rogel, E. Goldschmidt, A. K. Boddapati, H. Sohn, D. Sturdevant, J. W. Austin, L. Kardava, L. Yuesheng, P. Liu, S. Moir, S. K. Pierce, A. Madi, Shared transcriptional profiles of atypical B cells suggest common drivers of expansion and function in malaria, HIV, and autoimmunity. *Sci. Adv.* **7**, eabg8384 (2021).
25. N. Nath, R. Prasad, S. Giri, A. K. Singh, I. Singh, T-bet is essential for the progression of experimental autoimmune encephalomyelitis. *Immunology* **118**, 384–391 (2006).
26. J. I. Cohen, Epstein–Barr virus infection. *N. Engl. J. Med.* **343**, 481–492 (2000).
27. K. B. Fraser, J. H. D. Millar, M. Haire, S. Mccrea, Increased tendency to spontaneous in-vitro lymphocyte transformation in clinically active multiple sclerosis. *Lancet* **314**, 715–717 (1979).
28. A. Ascherio, K. L. Munger, Environmental risk factors for multiple sclerosis. Part I: The role of infection. *Ann. Neurol.* **61**, 288–299 (2007).
29. L. I. Levin, K. L. Munger, E. J. O'Reilly, K. I. Falk, A. Ascherio, Primary infection with the Epstein-Barr virus and risk of multiple sclerosis. *Ann. Neurol.* **67**, 824–830 (2010).
30. J. Pakpoor, G. Disanto, J. E. Gerber, R. Dobson, U. C. Meier, G. Giovannoni, S. V. Ramagopalan, The risk of developing multiple sclerosis in individuals seronegative for Epstein-Barr virus: A meta-analysis. *Mult. Scler.* **19**, 162–166 (2013).
31. H. B. Warner, R. I. Carp, Multiple sclerosis and Epstein-Barr virus. *Lancet* **2**, 1290 (1981).
32. S. Sheik-Ali, Infectious mononucleosis and multiple sclerosis—Updated review on associated risk. *Mult. Scler. Relat. Disord.* **14**, 56–59 (2017).
33. E. L. Thacker, F. Mirzaei, A. Ascherio, Infectious mononucleosis and risk for multiple sclerosis: A meta-analysis. *Ann. Neurol.* **59**, 499–503 (2006).
34. K. Bjornevik, M. Cortese, B. C. Healy, J. Kuhle, M. J. Mina, Y. Leng, S. J. Elledge, D. W. Niebuhr, A. I. Scher, K. L. Munger, A. Ascherio, Longitudinal analysis reveals high prevalence of Epstein-Barr virus associated with multiple sclerosis. *Science* **375**, 296–301 (2022).
35. A. Ascherio, K. L. Munger, E. T. Lennette, D. Spiegelman, M. A. Hernán, M. J. Olek, S. E. Hankinson, D. J. Hunter, Epstein-Barr virus antibodies and risk of multiple sclerosis: A prospective study. *JAMA* **286**, 3083–3088 (2001).
36. R. A. Farrell, D. Antony, G. R. Wall, D. A. Clark, L. Fisniku, J. Swanton, Z. Khaleeli, K. Schmierer, D. H. Miller, G. Giovannoni, Humoral immune response to EBV in multiple sclerosis is associated with disease activity on MRI. *Neurology* **73**, 32–38 (2009).
37. S. Cepok, D. Zhou, R. Srivastava, S. Nessler, S. Stei, K. Büssow, N. Sommer, B. Hemmer, Identification of Epstein-Barr virus proteins as putative targets of the immune response in multiple sclerosis. *J. Clin. Invest.* **115**, 1352–1360 (2005).
38. M. P. Pender, P. A. Csurhes, J. M. Burrows, S. R. Burrows, Defective T-cell control of Epstein–Barr virus infection in multiple sclerosis. *Clin. Transl. Immunol.* **6**, e126 (2017).
39. J. A. James, K. M. Kaufman, A. D. Farris, E. Taylor-Albert, T. J. Lehman, J. B. Harley, An increased prevalence of Epstein-Barr virus infection in young patients suggests a possible etiology for systemic lupus erythematosus. *J. Clin. Invest.* **100**, 3019–3026 (1997).
40. J. A. James, B. R. Neas, K. L. Moser, T. Hall, G. R. Bruner, A. L. Sestak, J. B. Harley, Systemic lupus erythematosus in adults is associated with previous Epstein-Barr virus exposure. *Arthritis Rheum.* **44**, 1122–1126 (2001).
41. Z.-X. Li, S. Zeng, H.-X. Wu, Y. Zhou, The risk of systemic lupus erythematosus associated with Epstein-Barr virus infection: A systematic review and meta-analysis. *Clin. Exp. Med.* **19**, 23–36 (2019).
42. N. Balandraud, J. B. Meynard, I. Auger, H. Sovran, B. Mugnier, D. Reviron, J. Roudier, C. Roudier, Epstein-Barr virus load in the peripheral blood of patients with rheumatoid arthritis: Accurate quantification using real-time polymerase chain reaction. *Arthritis Rheum.* **48**, 1223–1228 (2003).
43. P. B. Ferrell, C. T. Aitcheson, G. R. Pearson, E. M. Tan, Seroepidemiological study of relationships between Epstein-Barr virus and rheumatoid arthritis. *J. Clin. Invest.* **67**, 681–687 (1981).
44. M. A. Alspaugh, G. Henle, E. T. Lennette, W. Henle, Elevated levels of antibodies to Epstein-Barr virus antigens in sera and synovial fluids of patients with rheumatoid arthritis. *J. Clin. Invest.* **67**, 1134–1140 (1981).
45. A. C. Márquez, M. S. Horwitz, The role of latently infected B cells in CNS autoimmunity. *Front. Immunol.* **6**, 544 (2015).
46. A. Bar-Or, M. P. Pender, R. Khanna, L. Steinman, H.-P. Hartung, T. Maniar, E. Croze, B. T. Aftab, G. Giovannoni, M. A. Joshi, Epstein-Barr virus in multiple sclerosis: Theory and emerging immunotherapies. *Trends Mol. Med.* **26**, 296–310 (2020).
47. M. Olivadoti, L. A. Toth, J. Weinberg, M. R. Opp, Murine gammaherpesvirus 68: A model for the study of Epstein-Barr virus infections and related diseases. *Comp. Med.* **57**, 44–50 (2007).
48. C. Casiraghi, I. Shanina, S. Cho, M. L. Freeman, M. A. Blackman, M. S. Horwitz, Gammaherpesvirus latency accentuates EAE pathogenesis: Relevance to Epstein-Barr virus and multiple sclerosis. *PLOS Pathog.* **8**, e1002715 (2012).
49. C. Casiraghi, A. C. Márquez, I. Shanina, M. S. Horwitz, Latent virus infection upregulates CD40 expression facilitating enhanced autoimmunity in a model of multiple sclerosis. *Sci. Rep.* **5**, 13995 (2015).
50. K. M. Palaszynski, K. K. Loo, J. F. Ashouri, H. Liu, R. R. Voskuhl, Androgens are protective in experimental autoimmune encephalomyelitis: Implications for multiple sclerosis. *J. Neuroimmunol.* **146**, 144–152 (2004).
51. Y. Okuda, M. Okuda, C. C. A. Bernard, Gender does not influence the susceptibility of C57BL/6 mice to develop chronic experimental autoimmune encephalomyelitis induced by myelin oligodendrocyte glycoprotein. *Immunol. Lett.* **81**, 25–29 (2002).
52. B. E. Barnett, R. P. Staupe, P. M. Odorizzi, O. Palko, V. T. Tomov, A. E. Mahan, B. Gunn, D. Chen, M. A. Paley, G. Alter, S. L. Reiner, G. M. Lauer, J. Teijaro, E. J. Wherry, Cutting edge: B cell–intrinsic T-bet expression is required to control chronic viral infection. *J. Immunol.* **197**, 1017–1022 (2016).
53. Y. Liu, S. Zhou, J. Qian, Y. Wang, X. Yu, D. Dai, M. Dai, L. Wu, Z. Liao, Z. Xue, J. Wang, G. Hou, J. Ma, J. Harley, Y. Tang, N. Shen, T-bet^{+}CD11c^{+} B cells are critical for antichromatin immunoglobulin G production in the development of lupus. *Arthritis Res. Ther.* **19**, 225 (2017).
54. A. Mendoza, W. T. Yewdell, B. Hoyos, M. Schizas, R. Bou-Puerto, A. J. Michaels, C. C. Brown, J. Chaudhuri, A. Y. Rudensky, Assembly of a spatial circuit of T-bet–expressing T and B lymphocytes is required for antiviral humoral immunity. *Sci. Immunol.* **6**, eabi4710 (2021).
55. I. C. Mouat, I. Shanina, M. S. Horwitz, Age-associated B cells are long-lasting effectors that restrain reactivation of latent γHV68. bioRxiv 2021.12.29.474434 [**Preprint**]. 21 April 2022. https://doi.org/10.1101/2021.12.29.474434.
56. D. Lau, L. Y.-L. Lan, S. F. Andrews, C. Henry, K. T. Rojas, K. E. Neu, M. Huang, Y. Huang, B. DeKosky, A.-K. E. Palm, G. C. Ippolito, G. Georgiou, P. C. Wilson, Low CD21 expression defines a population of recent germinal center graduates primed for plasma cell differentiation. *Sci. Immunol.* **2**, eaai8153 (2017).
57. M. Matsumoto, A. Baba, T. Yokota, H. Nishikawa, Y. Ohkawa, H. Kayama, A. Kallies, S. L. Nutt, S. Sakaguchi, K. Takeda, T. Kurosaki, Y. Baba, Interleukin-10-producing plasmablasts exert regulatory function in autoimmune inflammation. *Immunity* **41**, 1040–1051 (2014).
58. I. C. Mouat, Z. J. Morse, I. Shanina, K. L. Brown, M. S. Horwitz, Latent gammaherpesvirus exacerbates arthritis through modification of age-associated B cells. *eLife* **10**, e67024 (2021).

59. K. Rubtsova, P. Marrack, A. V. Rubtsov, Age-associated B cells: Are they the key to understanding why autoimmune diseases are more prevalent in women? *Expert Rev. Clin. Immunol.* **8**, 5–7 (2012).
60. H. L. E. Lang, H. Jacobsen, S. Ikemizu, C. Andersson, K. Harlos, L. Madsen, P. Hjorth, L. Sondergaard, A. Svejgaard, K. Wucherpfennig, D. I. Stuart, J. I. Bell, E. Y. Jones, L. Fugger, A functional and structural basis for TCR cross-reactivity in multiple sclerosis. *Nat. Immunol.* **3**, 940–943 (2002).
61. T. V. Lanz, R. C. Brewer, P. P. Ho, J.-S. Moon, K. M. Jude, D. Fernandez, R. A. Fernandes, A. M. Gomez, G.-S. Nadj, C. M. Bartley, R. D. Schubert, I. A. Hawes, S. E. Vazquez, M. Iyer, J. B. Zuchero, B. Teegen, J. E. Dunn, C. B. Lock, L. B. Kipp, V. C. Cotham, B. M. Ueberheide, B. T. Aftab, M. S. Anderson, J. L. DeRisi, M. R. Wilson, R. J. M. Bashford-Rogers, M. Platten, K. C. Garcia, L. Steinman, W. H. Robinson, Clonally expanded B cells in multiple sclerosis bind EBV EBNA1 and GlialCAM. *Nature* **603**, 321–327 (2022).
62. E. Ricker, M. Manni, D. Flores-Castro, D. Jenkins, S. Gupta, J. Rivera-Correa, W. Meng, A. M. Rosenfeld, T. Pannellini, M. Bachu, Y. Chinenov, P. K. Sculco, R. Jessberger, E. T. L. Prak, A. B. Pernis, Altered function and differentiation of age-associated B cells contribute to the female bias in lupus mice. *Nat. Commun.* **12**, 4813 (2021).
63. S. A. Jenks, K. S. Cashman, E. Zumaquero, U. M. Marigorta, A. V. Patel, X. Wang, D. Tomar, M. C. Woodruff, Z. Simon, R. Bugrovsky, E. L. Blalock, C. D. Scharer, C. M. Tipton, C. Wei, S. S. Lim, M. Petri, T. B. Niewold, J. H. Anolik, G. Gibson, F. E.-H. Lee, J. M. Boss, F. E. Lund, I. Sanz, Distinct effector B cells induced by unregulated toll-like receptor 7 contribute to pathogenic responses in systemic lupus erythematosus. *Immunity* **49**, 725–739.e6 (2018).
64. M. P. Cancro, Age-associated B cells. *Annu. Rev. Immunol.* **38**, 315–340 (2020).

Acknowledgments: We are grateful to P. Marrack for providing *Tbx21*$^{fl/fl}$ and *Cd19*$^{cre/+}$ mice and the UBC LSI Flow Cytometry Core Facility and the UBC Modified Barrier Facility for assistance. The following reagent was obtained through the NIH Tetramer Core Facility: class II myelin oligodendrocyte glycoprotein tetramer. We express our gratitude to all the blood donors who participated in this study. **Funding:** This work was supported by Multiple Sclerosis Society of Canada grant 3631, Canadian Institutes of Health Research grants 462816 and 427030, University of British Columbia Four Year Doctoral Fellowship (to I.C.M.), endMS Doctoral Studentship Award (no. 2955 to J.R.A.), and endMS Doctoral Studentship Award (no. 900573 to N.M.F.). **Author contributions:** Conceptualization: I.C.M. and M.S.H. Methodology: I.C.M., I.S., J.R.A., N.M.F., and G.V. Investigation: I.C.M., J.R.A., N.M.F., V.F., A.M.G., I.S., and G.V. Visualization: I.C.M. Supervision: L.C.O., G.V., and M.S.H. Writing—original draft: I.C.M. and M.S.H. Writing—review and editing: J.R.A., N.M.F., L.C.O., and M.S.H. **Competing interests:** The authors declare that they have no competing interests. **Data and materials availability:** All data needed to evaluate the conclusions in the paper are present in the paper and/or the Supplementary Materials.

Submitted 31 August 2022
Accepted 26 October 2022
Published 25 November 2022
10.1126/sciadv.ade6844